



~100 nm wavelength tunable noise-like pulse based on two-dimensional parameter optimization of Tm-doped fiber laser

Desheng Zhao^{a,b}, Xiran Zhu^{c,d}, Jiawei Wang^{a,b}, Xiang Li^{a,b}, Zhiyuan Dou^e, Long Tian^{a,b,*}, Lirong Chen^{a,b}, Yaohui Zheng^{a,b,*}

^a State Key Laboratory of Quantum Optics and Quantum Optics Devices, Institute of Opto-Electronics, Shanxi University, Taiyuan 030006, China

^b Collaborative Innovation Center of Extreme Optics, Shanxi University, Taiyuan 030006, China

^c Beijing Institute of Tracking and Telecommunications Technology, Beijing 100094, China

^d Science & Technology on Integrated Information System Laboratory, Beijing 100094, China

^e Hunan Provincial Key Laboratory of Intelligent Sensors and Advanced Sensor Materials, School of Physics and Electronics, Hunan University of Science and Technology, Xiangtan 411201, China

ARTICLE INFO

Keywords:

Noise-like pulse
2 μm fiber laser
Wavelength tunable
Birefringent filter

ABSTRACT

We report a wavelength widely-tuned noise-like pulse (NLP) thulium-doped fiber laser. Free of additional filter, NLP with a wavelength tunable range of ~ 100 nm is realized by lowering the formation threshold power of NLP at different wavelengths and combining with intracavity birefringent filter. With the optimized two-dimensional intracavity parameters (gain fiber length of 2.9 m and single mode fiber length of 45 m), the NLP fiber laser achieves an adjustable wavelength from 1873.4 nm to 1969.3 nm (95.9 nm wavelength tunable range). The pulse width and average power of the NLP in the tuning range vary from 6.46 ns to 16.86 ns and from 0.211 W to 0.355 W, respectively. To our knowledge, this is the widest wavelength tunable NLP fiber laser, capable of variety applications in optical coherence tomography, material processing, imaging and so on.

1. Introduction

Over recent years, the unique properties of noise-like pulse (NLP) mode-locking fiber lasers have drawn extensive attention from researchers [1–3]. In contrast to conventional pulse patterns, NLP is bundled by a significant number of solitons with arbitrary amplitude and phase [4,5], which makes them low-coherent and wide envelope. These properties enable it to realize high power by a simple main oscillator power amplification structure, and this permits applications in the material processing and optical coherence tomography (OCT) [6]. Besides, the high peak power soliton pulses within the NLP envelope can provide significant advantages in spectral manipulation of the mid-infrared supercontinuum [7,8].

The excellent properties of NLP are of deeper interest to researchers, including high order mode [9,10], new wavelength bands [11,12], wavelength tunability [13] and so on [14]. In particular, the wavelength tunable feature offers a broader application prospect for NLP, which is of great value in the fields of fiber sensing, nonlinear frequency conversion, and low-coherence spectral interferometry. Wavelength tunable NLP

fiber lasers are generally obtained based on different filtering mechanisms in 2 μm waveband. By inserting spatial filter elements into the cavity, Tokurakawa et al. realized NLPs with wavelength tuning from 1895 nm to 1942 nm, corresponding to a tuning range of 47 nm [15]. However, the use of spatially structured filter element destroys the advantages of all-fiberized laser. Zhao et al. obtained NLPs with a continuously tunable range of 46.9 nm by utilizing the intracavity optimized birefringent filtering mechanism [16]. Based on the temperature control of the PM2000D fiber in the cavity, Zheng et al. enabled the center wavelength of the NLP to be tuned from 1910.4 nm to 1942.8 nm, and the tuning range of the NLP is 32.4 nm [17]. However, the use of special fiber in the cavity increases the intracavity splicing loss. Especially when the pulse undergoes multiple cycles in the cavity, the intracavity loss cannot be negligible and will limit the expansion of the wavelength tunable range. Besides intracavity loss, the gain and nonlinearity required for NLP formation directly affects the establishment of mode-locking at different wavelengths, limiting the range of the wavelength tunable NLP. Therefore, in order to obtain NLPs with a wider tuning range (compared to the studies of wavelength tunable NLP

* Corresponding authors at: State Key Laboratory of Quantum Optics and Quantum Optics Devices, Institute of Opto-Electronics, Shanxi University, Taiyuan 030006, China.

E-mail addresses: tianlong@sxu.edu.cn (L. Tian), yhzheng@sxu.edu.cn (Y. Zheng).

<https://doi.org/10.1016/j.infrared.2024.105678>

Received 8 October 2024; Received in revised form 1 December 2024; Accepted 15 December 2024

Available online 21 December 2024

1350-4495/© 2024 Elsevier B.V. All rights reserved, including those for text and data mining, AI training, and similar technologies.

to date), it is necessary to investigate the effect of NLP formation at different wavelengths. Unfortunately, the majority of current literatures focuses on the investigation of filtering mechanism to obtain wavelength tunable NLP.

In this paper, we realize a wavelength broadband tunable NLP based on the birefringence filtering effect in a thulium-doped fiber laser. To maximize the wavelength tuning range, the gain and nonlinearity in the cavity are manipulated to reduce the mode-locking threshold power of NLP. This is achieved by intracavity gain fiber and single mode fiber (SMF) lengths optimization. With an optimized thulium-doped fiber (TDF) length of 2.9 m and a SMF length of 45 m, wavelength tuning of the NLP from 1873.4 nm to 1969.3 nm is achieved by controlling the intracavity polarization state and the injected power. The wavelength tuning range of the NLP is up to 95.9 nm, the widest tuning range reported for an NLP fiber laser.

2. Experiment structure

The experimental structure of the wavelength tunable NLP fiber laser based on intracavity birefringence filtering effect is illustrated in Fig. 1. A commercially available fiber laser with an output power of 5 W and a central wavelength of 1550 nm pumps a section of TDF (9/125 μm , 0.15 numerical aperture) to provide gain in 2 μm band. The pump laser is injected into the cavity through a fused wavelength-division multiplexer (WDM) with a power handling of 5 W. A piece of SMF (8/125 μm , 0.14 numerical aperture) is fused to the gain fiber to provide the nonlinearity required for NLP realization. The gain fiber and SMF lengths are optimized to 2.9 m and 45 m, respectively. A 2000 nm optical coupler (OC 1) with a coupling ratio of 50:50 connects the left and right rings to form nonlinear amplifying loop mirror (NALM) mode-locking. In the right ring, an isolator (ISO) is used to force the laser to transmit in a clockwise direction. A 50 % output port of the OC 2 extracts power from the cavity. Since intracavity birefringent filtering effects as well as mode-locking establishment require the regulation of the intracavity polarization state, two polarization controllers (PCs) are inserted into the fiber laser. The total length of the gain fiber, the passive fiber, and the pigtailed of the fiber components within the entire laser is 54.8 m, corresponding to the pulse repetition frequency of 3.64 MHz.

To characterize the spectrum of the pulse emitted from the fiber laser, an optical spectrum analyzer (AQ6375B) with a scanning range of 1200 nm-2400 nm is used. The time-domain information is obtained by a high-speed oscilloscope (DSOS404A) with a bandwidth of 4 GHz. The radio frequency (RF) information and autocorrelation (AC) trace are obtained by a signal & spectrum analyzer (R&S FSW8) with a bandwidth of 8 GHz and an autocorrelator (APE 50) with a scanning range of 50 ps, respectively.

3. Experimental results and discussions

The fiber laser allows the excitation of continuous wave with center wavelength of 1885 nm to the maximum injected power when the polarization state of the cavity is not altered. Stable mode-locking pulse trains are obtained by setting the injected power of the fiber laser to 1.1

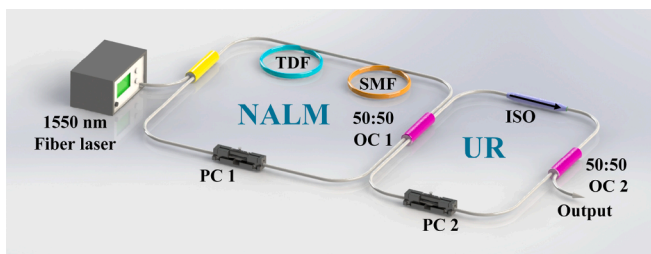


Fig. 1. The experimental structure of wavelength tunable NLP fiber laser.

W in combination with rotating and squeezing PCs. As the injected power is continuously increased, the mode-locking pulse remains a stable state without pulse wave breaking and mode-locked losing phenomenon occur. The pulse evolution with injected power is characterized in Fig. 2, where the variations of the pulse spectra, waveforms, AC traces and power are plotted separately. After the injected power reaches the mode-locking threshold power, the pulse center wavelength and 3-dB spectral width are 1891.8 nm and 10.5 nm, respectively. The spectral dips appear on the spectrum due to the strong water absorption lines in the atmosphere. As the injected power increases to 5 W, the spectrum intensity increases, and the pulse waveform linearly broadens to 14.58 ns. As illustrated in Fig. 2(c), a spike signal on the AC trace is obtained by using an autocorrelator. The wide spectral range, nano-second waveform, and spike signal on the AC trace indicate that the designed laser is an NLP mode-locking fiber laser [18,19]. The spike intensity enhances, and the width gradually decreases with the rising of the injected power. At an injection power of 5 W, the full width at half maximum of the spike is 1.17 ps and the corresponding duration is 830 fs, signifying the average duration of the soliton pulse within the NLP envelope [20]. In general, the AC trace of the NLP is organized on a dual scale, in our experiments, it is difficult to observe the actual AC traces of NLPs since the actual pedestal width of the obtained NLPs is > 50 ps. The output power of the NLP is gradually increased to 262 mW due to higher gain provided in the fiber laser. The corresponding slope and conversion efficiencies are 5.5 % and 5.2 %, respectively.

Fig. 3(a) and 3(b) show the RF spectral information of the NLP within 50 MHz and 1 MHz range. As the injected power is increased from 1.1 W to 5 W, periodic modulation appears in the RF spectrum. The modulation bandwidth is an inverse proportion of the pulse width, therefore the modulation bandwidth is about 69.1 MHz at the maximum injected power. The signal-to-noise ratio of the NLP is 58.9 dB at this injected power level. The repetition frequency of the NLP is 3.64 MHz, indicating that the round trip time of the pulse is 274.7 ns. Due to the random fluctuation of subpulses within the NLP, sidelobes appear in the spectrum of the NLP.

Benefiting from the intracavity birefringent filtering effect, the wavelength tunable capability of the fiber laser is achieved by controlling the intracavity polarization state. Fig. 4 demonstrates the wavelength tuning process of the NLP at maximum injection power. The NLP is tuned from 1873.4 nm to 1969.3 nm by rotating and squeezing the PCs. The corresponding tuning range is 95.9 nm, the widest NLP tuning range that has been reported in the literatures. The formation of birefringent filter is attributed to the birefringence of the fiber in the cavity. The combination of the fibers and the PCs on the fiber forms an invisible birefringent filter in the cavity. Although the length of the intracavity fiber is limited, the bends in the fiber and the stresses exerted by the PCs on the fiber induce a significant amount of birefringence. Sufficient birefringence ensures the achievement of wavelength tunable NLP based on the birefringence filtering effect. The wavelength tunability of the NLP at short and long wavelengths is realized by manually rotating and squeezing PC 1 and PC 2.

The variations of average power and pulse width of the NLP over the wavelength tuning range are displayed in Fig. 4(b). As the center wavelength of NLP tuning from shortwave to longwave, the average power and pulse width of the NLP change from 211 mW to 355 mW and 6.46 ns to 16.86 ns, respectively. On the one hand, when the intracavity polarization state is tuned, the different intracavity losses make the net gain distribution and intensity in the cavity vary, and the energy obtained by the mode-locked pulses at different wavelengths circulating in the cavity is different. On the other hand, the intracavity birefringence is changed when the polarization state is adjusted, and thus, the nonlinear phase shifts induced by fiber birefringence are different, combining with the different gain at different wavelengths to cause the variations in the average power and pulse width. Furthermore, accurate wavelength tuning repeatability is possible by using electronically controlled PCs.

In the experiment, the formation of NLP mode-locking at different

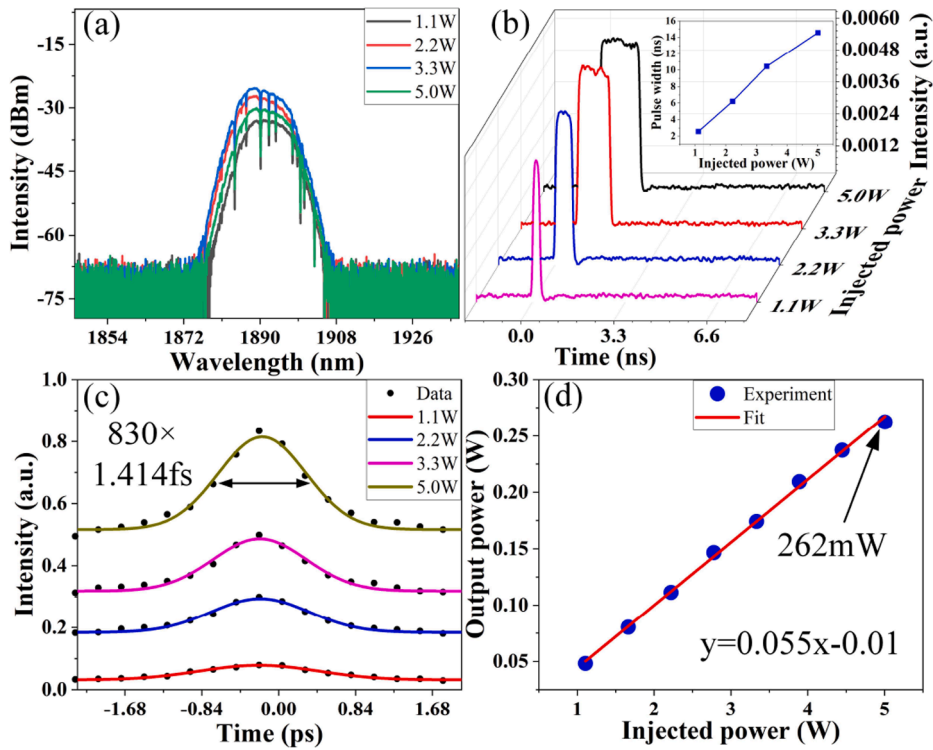


Fig. 2. The (a) spectra, (b) pulse waveforms, (c) AC traces and (d) power of the mode-locking pulse evolve with the injected power.

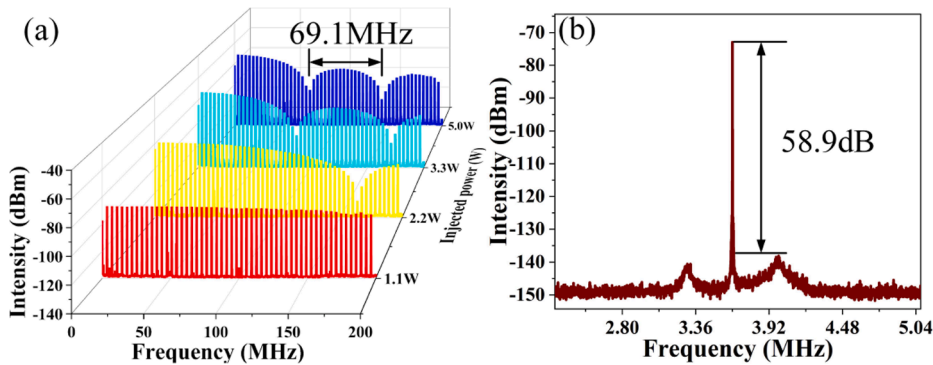


Fig. 3. (a) The RF spectral evolution with injected power. (b) The RF spectrum at maximum injected power.

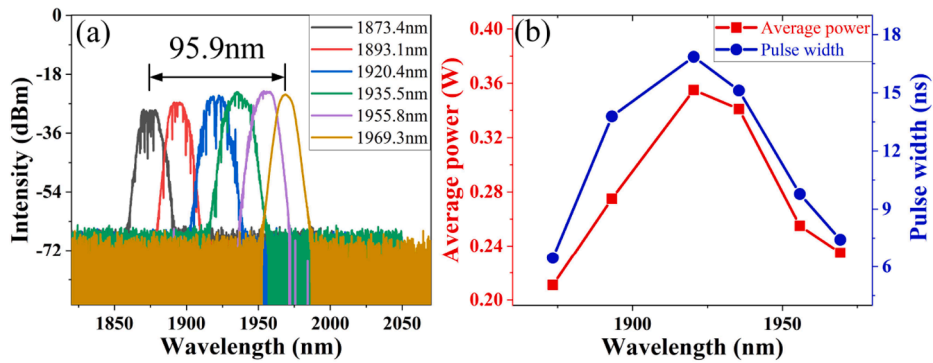


Fig. 4. (a) The NLP spectra in the wavelength tuning range. (b) Variation of average power and pulse width with wavelength.

wavelengths affects the expansion of the wavelength tuning range, which is related to the cavity's multi-dimensional parameters. In the experiments, the effects of two-dimensional parameters (the passive

fiber length and gain fiber length) on the tuning range are investigated. Except for the alterations of the fiber length and the polarization state in the cavity, all other cavity parameters remain unchanged, and the

injected power is set to its maximum value. The effect of altering the passive fiber length on the wavelength tuning range of the NLP is displayed in Fig. 5. When the SMF length is shorter than 15 m, the high mode-locking threshold power makes it impossible to establish the NLP in a stable state. A tuning range of 35.4 nm is obtained by adjusting the PCs with the 15 m SMF inserted into the cavity. The wavelength tuning range of NLP increases to 95.9 nm with increasing the intracavity SMF length to 45 m. Due to the increase in the length of the SMF, more nonlinear phase shifts are induced, leading to a reduction in the mode-locking threshold power for both shorter and longer wavelengths. However, the further expansion of the SMF length increases the intracavity loss, disfavoring the expansion of the tuning range of NLP. As a result, the wavelength tuning range is only 63 nm at 65 m SMF. Comparison of the NLP's pulse widths in the tuning range for different SMF lengths is plotted in Fig. 5(b). The increase in SMF length leads more intracavity nonlinearity, broadening the widths of the mode-locking pulse and causing the maximum pulse width to increase from 2.546 ns to 19.627 ns. However, the introduction of SMF also leads to more loss in the cavity and reduces the output power of the fiber laser. As illustrated in the Fig. 5(c), the maximum average power of the NLP at 15 m SMF length is higher than that of the NLP at other lengths in the fiber laser.

Fig. 6(a) exhibits the NLP wavelength tuning range for gain fiber lengths of 1.9 m, 2.9 m and 5 m lengths. As the TDF length increases from 1.9 m to 2.9 m, the increase in intracavity gain ensures that mode-locking can be achieved at shorter and longer wavelengths, resulting in a longer adjustment range. Thus, the center wavelength of the NLP is blue-shifted from 1923.5 nm to 1873.4 nm as well as red-shifted from 1965.4 nm to 1969.3 nm, with a corresponding increase in the tuning range from 43.1 nm to 95.9 nm. Further using a longer gain fiber (i.e., 5 m), the central wavelength of the NLP extends to longer wavelength because the reabsorption effect of the gain fiber providing gain at longer wavelength [21]. As a result, the fiber laser can be achieved mode-locking at 1975.2 nm (1969.3 nm at 2.9 m TDF). However, the loss introduced by the reabsorption process makes it difficult to achieve NLP mode-locking at shorter wave. The shortest wave is red-shifted from 1873.4 nm to 1914.8 nm and the corresponding NLP tuning range is reduced to 61 nm at 5 m TDF. Comparisons of the pulse widths and average power of the NLP for different tuning ranges are displayed in Fig. 6(b) and 6(c). Since NLP formation demands a specific peak power, low intracavity gain requires NLP to achieve an increase in peak power by decreasing the pulse width. Therefore, the narrowest NLP pulse width is obtained from the fiber laser at 1.9 m TDF. Increasing the gain fiber length to 2.9 m allows the pulse width of the NLP in the tuning range varying from 6.46 ns to 16.86 ns, which is broader than the pulse width of the NLP at short gain fiber length (from 3.53 ns to 3.9 ns). With sufficient gain in the cavity configuration, the pulse is able to achieve start-up with a low mode-locking threshold power. As the injected power increases further, the peak power clamping effect of the intracavity NLP forces the pulse to broaden the pulse width to preserve a constant peak power in the cavity. Therefore, the pulse width of the NLP at 2.9 m gain fiber length is greater than the pulse width at 1.9 m. Inserting longer gain fiber into the fiber

laser, the increase in intracavity loss limits the extent of NLP broadening under the influence of peak power clamping effect, resulting in a maximum pulse width of only 12.86 ns in the wavelength tuning range. Due to the increased reabsorption loss introduced by the extended length of the gain fiber, the maximum power (0.355 W) of the NLP is obtained at 1.9 m TDF.

The wavelength tunable capability of mode-locking fiber laser can be achieved by using tunable filter, Lyot filter, birefringent filter and other filter schemes [22–26]. The tunable filter allows for hundreds of nm tuned mode-locking pulse and continuous wave [27,28], but its narrow bandwidth of tunable filter limits the formation and tuning range of NLP. The fusion loss between different type fibers is not ignorable when the polarization-maintaining fiber-based Lyot filter is inserted into the cavity, which introduces more insertion loss, limits the wavelength tunable range of the pulse and breaking the unique advantages of an all-fiberized structure. In contrast, the birefringent filter removes the need to introduce additional filter elements into the fiber laser and reduces intracavity loss as well as high-cost efficiency. Combining its flexible and variable bandwidth facilitates the realization of a broadband wavelength tunable range for NLP. Therefore, the intracavity birefringent filter is used as a key element for broadband tunability of NLP wavelength. To achieve the widest wavelength tunable NLP, the lengths of the gain fiber and the passive fiber are experimentally optimized. A comparison of the NLP wavelength ranges with different gain fiber lengths reveals that a broadband tunable NLP is only obtained with a moderate gain fiber length. Too short or too long gain fiber lengths limit the expansion of the wavelength tuning range.

Different from the general conditions for mode-locked pulse formation (i.e., conventional soliton, dispersion-managed soliton, and dissipative soliton), the formation of NLP does not depend on the regulation of intracavity dispersion, which can be formed in both normal- and anomalous-dispersion regimes. The gain and passive fibers we used exhibit large anomalous dispersion at 2 μm , so the fiber laser operates in the net anomalous dispersion region. In the anomalous dispersion regime, the formation of NLP is associated with soliton collapse and intracavity positive feedback [29]. Also, sufficient nonlinearity is required for the formation of NLP. In 2 μm band, mode-locking and wavelength tunability can be achieved by inserting ultra-high numerical aperture fiber, SMF, SM1950 and specialty fibers into the cavity [30–32]. Based on the normal dispersion and nonlinearity of UHNAF, the insertion of UHNAF in thulium-doped fiber laser is favorable for the formation of NLP and the realization of wavelength tunability. However, the UHNAF has a small core and a large numerical aperture introduces high fusion loss into the cavity, limiting its integration with fiber components and gain fibers. Compared with SM1950 fibers, SMF has the advantage of cost effectiveness. The fusion loss of the SMF to the fiber components and gain fibers used in the cavity can be minimized. By optimizing the length of the SMF inserted in the cavity, an NLP wavelength tuned range of 95.9 nm is obtained. Table 1 summarizes the published literature on NLP wavelength tuning range. It can be clearly seen that the widest tuning range of NLP is realized based on intracavity

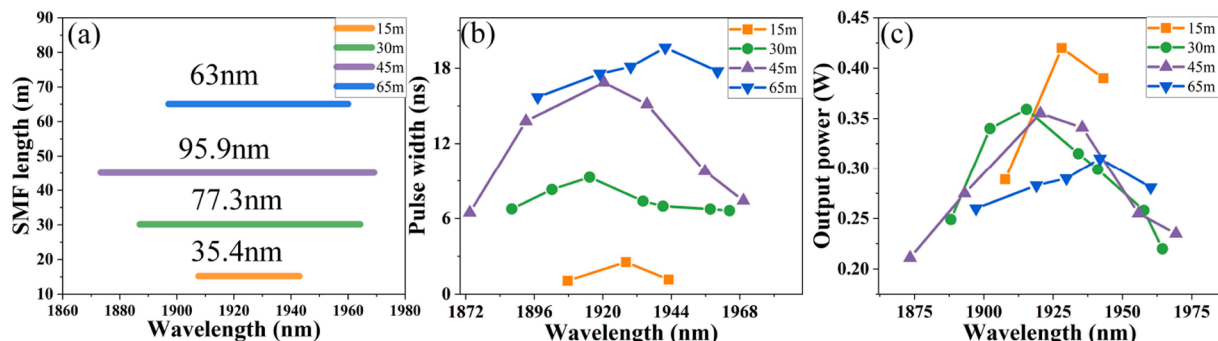


Fig. 5. The wavelength tunable range under different SMF lengths. Comparison of the (b) pulse width and (c) output power of fiber laser with different fiber lengths.

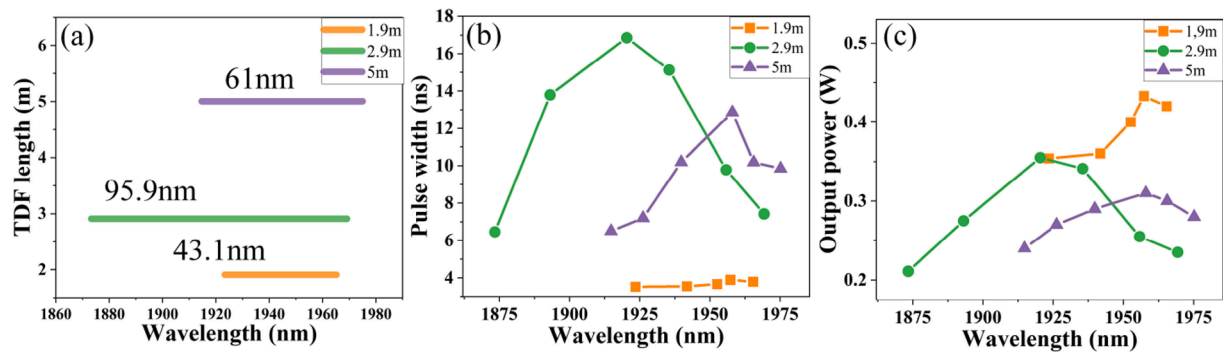


Fig. 6. (a) The realized NLPs with different central wavelengths at TDF lengths of 1.9 m, 2.9 m, and 5 m, respectively. (b) The pulse width and (c) output power at different NLP center wavelengths and TDF lengths.

Table 1

Comparison of wavelength-tuned NLP fiber laser.

Mode-locked technique	Realization method	Tuning range	Dopant	Reference
Fiber loop mirror	Comb filter	53 nm	Er	[33]
Semiconductor saturable absorber mirror	Telescope lense	47 nm	Tm	[15]
Semiconductor saturable absorber mirror	Tunable filter	57 nm	Er	[34]
NALM	Birefringent filter	46.9 nm	Tm/ Ho	[16]
Nonlinear optical loop mirror	Temperature control	32.4 nm	Tm	[17]
Nonlinear polarization rotation + NALM	Nonlinear polarization rotation	41 nm	Er	[35]
NALM	Birefringent filter	95.9 nm	Tm	This work

birefringent filtering effect in this work. Further extension of the wavelength tuning range is possible from the following directions: on the one hand, intracavity loss is reduced by using SM1950 or SM2000 fibers with lower transmission loss as the intracavity passive fibers as well as the pigtails of the fiber components, while ignoring the cost of the fiber laser. On the other hand, the cavity gain needs to be increased, which is achieved either by using a bidirectional pumping scheme or by using highly thulium-doped fiber with higher gain.

4. Conclusion

In conclusion, we have reported a broadband wavelength-tuned NLP thulium-doped fiber laser by employing low-cost intracavity birefringent filter as a key component for NLP wavelength tunability. The intracavity gain and nonlinearity are manipulated by optimizing the intracavity gain fiber and passive fiber lengths to lower the mode-locking formation threshold power, thus obtaining broadband wavelength tunable NLP. At the maximum available pump power of the thulium-doped fiber laser, an NLP with wavelength tuned from 1873.4 nm to 1969.3 nm is achieved. The corresponding tunned wavelength range is 95.9 nm, the widest wavelength tunable NLP to the best of our knowledge. The maximum pulse width and average power of the NLP within the wavelength tuning range are 16.86 ns and 355 mW, respectively. Such a widely wavelength tuning range of NLP enables important role in fiber sensing, imaging, etc.

CRediT authorship contribution statement

Desheng Zhao: Writing – review & editing, Writing – original draft, Visualization, Conceptualization. **Xiran Zhu:** Writing – review &

editing, Validation, Supervision. **Jiawei Wang:** Investigation, Conceptualization. **Xiang Li:** Validation, Data curation. **Zhiyuan Dou:** Visualization, Conceptualization. **Long Tian:** Project administration, Investigation, Data curation. **Lirong Chen:** Visualization, Funding acquisition, Conceptualization. **Yaohui Zheng:** Writing – review & editing, Resources.

Declaration of competing interest

The authors declare that they have no known competing financial interests or personal relationships that could have appeared to influence the work reported in this paper.

Acknowledgement

This work was supported by the National Natural Science Foundation of China (NSFC) (Grants No. 62225504, No. U22A6003, No. 62035015).

Data availability

Data will be made available on request.

References

- [1] Z. Wang, H. Pan, H. Chu, Z. Pan, Y. Li, S. Zhao, D. Li, Ultrafast nonlinear optical response of layered violet phosphorus for femtosecond noise-like pulse generation, *Opt. Express* 32 (2024) 15472–15482.
- [2] Y. Zhang, K. Wu, Z. Guang, B. Guo, D. Qiao, Z. Wei, H. Yang, Q. Wang, K. Li, N. Copner, X. Li, Advances and Challenges of Ultrafast Fiber Lasers in 2–4 μm Mid-Infrared Spectral Regions, *Laser Photonics Rev.* 18 (2024) 2300786.
- [3] M. Wang, D. Ouyang, Y. Lin, Y. Chen, M. Liu, J. Zhao, X. Liu, S. Ruan, Efficient Pulsed Raman Laser with Wavelength above 2.1 μm Pumped by Noise-Like Pulse, *Adv. Photonics Res.* (2024) 2300342.
- [4] L. Yu, J. Liang, Z. Tang, Q. Zeng, J. Wang, J. Wang, X. Luo, P. Yan, F. Dong, X. Liu, Q. Lue, C. Guo, S. Ruan, Generation of Mid-Infrared Noise-Like Pulses from a Polarization-Maintaining Fluoride Fiber Oscillator, *Adv. Photonics Res.* 4 (2023) 2300135.
- [5] Y. Zhou, X. Chu, Y. Qian, C. Liang, A. Komarov, X. Tang, M. Tang, H. Zhu, L. Zhao, Investigation of noise-like pulse evolution in normal dispersion fiber lasers mode-locked by nonlinear polarization rotation, *Opt. Express* 30 (2022) 35041–35049.
- [6] S. Kobtsev, A. Komarov, Noise-like pulses: stabilization, production, and application, *JOSA B* 41 (2024) 1116–1127.
- [7] X. Zhu, D. Zhao, B. Zhang, L. Yang, J. Yao, Y. Yang, S. Liu, J. Hou, Spectrally flat mid-infrared supercontinuum pumped by a high power 2 & #x00B5;m noise-like pulse, *Opt. Express* 31 (2023) 13182–13194.
- [8] X. Luo, Y. Tang, F. Dong, J. Wang, L. Yu, P. Yan, J. Wang, Z. Zheng, Q. Lue, C. Guo, All-fiber mid-infrared supercontinuum generation pumped by ultra-low repetition rate noise-like pulse mode-locked fiber laser, *J. Lightwave Technol.* 40 (2022) 4855–4862.
- [9] D. Xing, J. He, P. Wang, K. Chang, C. Liu, Y. Liu, Z. Wang, Transition between noise-like pulses and Q-switching in few-mode mode-locked lasers, *Opt. Express* 30 (2022) 20076–20087.
- [10] G. Xu, J. Peng, H. Zhang, Y. Zhang, M. Cui, Y. Su, Y. Zheng, All-multimode fiber spatiotemporal mode-locked figure-eight laser based on multimode gain fiber, *Opt. Express* 31 (2023) 44603–44610.

- [11] K.Y. Lau, S. Firstov, Z. Luo, M. Hu, A. Senatorov, A. Umnikov, B. Xu, X. Liu, J. Qiu, 1450 nm high energy noisy multi-pulse mode-locking in bismuth-doped fiber laser, *J. Lightwave Technol.* (2023).
- [12] D. Zhao, X. Zhu, S. Liu, L. Jiang, X. Yang, Y. Bu, B. Zhang, J. Hou, 1.35 μ J, 5.33 W Noise-Like Pulse Emission From an All-Polarization Maintaining Holmium-Doped Fiber Laser System, *J. Lightwave Technol.* 42 (2024) 5004–5008.
- [13] C. Gao, L. Dai, Q. Huang, K. Li, M. Fan, Q. Song, Z. Yan, F. You, X. Sun, C. Mou, Wavelength-tunable noise-like fiber laser based on PbS quantum dot saturable absorber film, *Appl. Opt.* 61 (2022) 5172–5178.
- [14] K. Li, X. Wang, X. Geng, M. Lu, M. Fu, Y. Fan, S. Li, Real-time observation of stationary and pulsating noise-like vector pulses in a fiber laser, *Opt. Express* 31 (2023) 23406–23418.
- [15] Y. Mashiko, E. Fujita, M. Tokurakawa, Tunable noise-like pulse generation in mode-locked Tm fiber laser with a SESAM, *Opt. Express* 24 (2016) 26515–26520.
- [16] D. Zhao, B. Zhang, S. Liu, X. Zhu, Z. Dou, L. Yang, J. Hou, Wavelength switchable and tunable noise-like pulses from a 2 μ m figure-eight all-fiber laser, *Opt. Laser Technol.* 150 (2022) 107942.
- [17] Y. Zhang, Y. Zheng, X. Su, H. Zhang, T. Sun, M. Cui, J. Peng, Wavelength tunable all-polarization-maintaining fiber laser at 2 μ m, *Opt. Laser Technol.* 168 (2024) 109850.
- [18] J. Huang, J. Lin, Y. Xie, X. Zhang, Generation and breakage of noise-like square pulses in a Tm-doped figure-8 fiber laser, *Infrared Phys. Technol.* 129 (2023) 104569.
- [19] D. Zhao, X. Zhu, S. Liu, L. Jiang, X. Yang, Y. Bu, B. Zhang, J. Hou, 1.35 μ J, 5.33 W noise-like pulse emission from an all-polarization maintaining holmium-doped fiber laser system, *J. Lightwave Technol.* (2024).
- [20] X. Zhu, D. Zhao, B. Zhang, Q. Jiang, L. Yang, L. Jiang, Y. Bu, Y. Yang, J. Hou, Ultra-flat and high-efficient mid-infrared supercontinuum generation in indium fluoride fiber, *Infrared Phys. Technol.* 137 (2024) 105115.
- [21] L. Zhang, J. Zhang, Q. Sheng, Y. Li, C. Shi, W. Shi, J. Yao, 1.7- μ m Tm-doped fiber laser intracavity-pumped by an erbium/ytterbium-codoped fiber laser, *Opt. Express* 29 (2021) 25280–25289.
- [22] H. Zhang, D. Tang, R.J. Knize, L. Zhao, Q. Bao, K.P. Loh, Graphene mode locked, wavelength-tunable, dissipative soliton fiber laser, *Appl. Phys. Lett.* 96 (2010).
- [23] Y. Han, L. Liu, Q. Li, Y.-Y. Li, H.-L. Wen, L.-Y. Zhou, G. Wu, C.-Y. Ma, B. Gao, Tunable and switchable multi-wavelength mode-locked fiber lasers induced by an optimized hybrid mode-locked composite filtering effect, *Opt. Express* 32 (2024) 27906–27918.
- [24] G. Ye, B. Liu, M. Dai, Y. Ma, T. Shirahata, S. Yamashita, S.Y. Set, Pump-power-controlled L-band wavelength-tunable mode-locked fiber laser utilizing nonlinear polarization evolution in all-polarization-maintaining fibers, *Opt. Lett.* 49 (2024) 2433–2436.
- [25] Q. Zeng, Z. Tang, D. Ouyang, L. Yu, J. Wang, X. Luo, W. Dong, P. Yan, J. Wang, P. Wang, Q. Lue, C. Guo, S. Ruan, Wavelength-tunable spatiotemporal mode-locking in a large-mode-area Er:ZBLAN fiber laser at 2.8- μ m, *Opt. Lett.* 49 (2024) 1117–1120.
- [26] G. Gao, S. Wang, Q. Zhao, Z. Cong, Z. Liu, Z. Zhao, Consecutive 1015–1105-nm wavelength tunable “figure-of-9” mode-locked Yb: fiber oscillator, *Opt. Lett.* 47 (2022) 5869–5872.
- [27] R. Dai, Y. Meng, Y. Li, J. Qin, S. Zhu, F. Wang, Nanotube mode-locked, wavelength and pulsewidth tunable thulium fiber laser, *Opt. Express* 27 (2019) 3518–3527.
- [28] M. Sabra, B. Leconte, D. Darwich, R. Dauliat, T. Tiess, R. Jamier, G. Humbert, M. Jäger, K. Schuster, P. Roy, Widely Tunable Dual-Wavelength Fiber Laser in the 2 μ m Wavelength Range, *J. Lightwave Technol.* 37 (2019) 2307–2310.
- [29] D. Tang, L. Zhao, B. Zhao, Soliton collapse and bunched noise-like pulse generation in a passively mode-locked fiber ring laser, *Opt. Express* 13 (2005) 2289–2294.
- [30] P. Hu, J. Mao, X. Zhou, T. Feng, H. Nie, R. Wang, B. Zhang, T. Li, J. He, K. Yang, Multiple soliton mode-locking operations of a Holmium-doped fiber laser based on nonlinear polarization rotation, *Opt. Laser Technol.* 161 (2023) 109218.
- [31] S. Filatova, V. Kamynin, D. Korobko, A. Fotiadi, A. Lobanov, A. Zverev, P. Balakin, Y. Gladush, D. Krasnikov, A. Nasibulin, V. Tsvetkov, Experimental and numerical study of different mode-locking techniques in holmium fiber laser with a ring cavity, *Opt. Express* 32 (2024) 22233–22248.
- [32] Y. Wu, Z. Dong, L. Hua, Z. Zhang, J. Tian, Y. Song, Improvement of peak power of dissipative soliton resonance pulse in a thulium-doped fiber laser, *Opt. Laser Technol.* 157 (2023) 108656.
- [33] J. Lin, Z. Dong, T. Dong, Y. Zhang, C. Dai, P. Yao, C. Gu, L. Xu, All-fiber figure-eight wavelength-tunable noise-like pulse lasers, *Opt. Laser Technol.* 141 (2021) 107146.
- [34] J. Li, C. Wang, P. Wang, Tunable noise-like pulse and Q-switched erbium-doped fiber laser, *Opt. Express* 30 (2022) 4768–4781.
- [35] Y.-N. Zhao, B. Gao, H. Di, J.-Y. Huo, L.-Y. Zhou, Y. Han, G. Wu, L. Liu, Wavelength tunable noise-like pulses in a hybrid mode-locked erbium-doped fiber laser, *Opt. Fiber Technol.* 87 (2024) 103893.